

Research Article

Statistical Analysis of Quenching & Partitioning Effects on Mechanical Properties of 1.7102 Steel Using ANOVA Technique

A.A. Abedini¹, H. Rastegari¹, S.M. Emam^{2*} and S.M.H. Seyedkashi³¹Department of Mechanical and Materials Engineering, Birjand University of Technology, Birjand, Iran²Department of Mechanical Engineering, Faculty of Engineering, Ardakan University, P.O. Box 184, Ardakan, Iran³Mechanical Engineering Department, University of Birjand, Birjand 97175-376, Iran

ARTICLE INFO

Article history:

Received 26 September 2024

Reviewed 30 November 2024

Revised 24 December 2024

Accepted 29 December 2024

Keywords:

Quenching and partitioning

1.7102 steel

Mechanical properties

Analysis of variance

Please cite this article as:

Abedini, A. A., Rastegari, H., Emam, S. M., & Seyedkashi, S. M. H. (2024). Statistical analysis of quenching & partitioning effects on mechanical properties of 1.7102 steel using ANOVA technique. *Iranian Journal of Materials Forming*, 11(4), 4-17. <https://doi.org/10.22099/ijmf.2025.51281.1303>

ABSTRACT

Quenched and partitioned (Q&P) steels represent a new generation of advanced high-strength steels, characterized by their excellent combination of strength and ductility. The high ductility of Q&P steels is attributed to their unique micro-composite microstructure, consisting of a martensitic matrix and 10-15% residual austenite. This research aims to determine the process parameters and investigate their effect on the ultimate tensile strength, yield strength, total elongation, reduction of area, and hardness of 1.7102 silicon medium carbon steel specimens subjected to quenching and partitioning processes. A full factorial design of experiments (DOE) was obtained using Minitab software for statistical analysis of the results. First, the normality of data was validated, and the main effects and interactions were analyzed through analysis of variance (ANOVA). The findings reveal that quenching temperature, partitioning time, and their interaction had a significant effect on the response.

© Shiraz University, Shiraz, Iran, 2024

1. Introduction

The primary focus of the automotive industry has always been to design vehicles that are faster, safer, and emit less carbon dioxide [1-3]. To improve automobile performance, ongoing effort focuses on developing new types of steel to reduce vehicle weight, enhance

passenger safety, and reduce fuel consumption. Accordingly, designing new materials in this process is a top priority. To address these challenges, researchers have been exploring advanced high-strength steels (AHSS), which offer a beneficial combination of strength and ductility due to their multi-phase

* Corresponding author

E-mail address: sy.m.emam@ardakan.ac.ir (S.M. Emam)<https://doi.org/10.22099/ijmf.2025.51281.1303>

microstructure. AHSS steels are classified into three generations [4]. The first generation is ferritic steels with limited ductility, including dual-phase steels (DP), plasticity caused by martensitic transformation (TRIP), multiphase (CP), and martensitic steels. The second generation includes austenite-based steels, which are known for their superior ductility but are relatively expensive due to their alloy elements and high processing costs [5, 6]. This category includes austenitic stainless steels, twinning-induced plasticity (TWIP), and lighter steels with induced plasticity.

The third generation of steels (high-strength low-alloy (HSLA)) includes materials with intermediate properties between the first and second generations, which are formed by performing the new heat treatment process (Q&P) on the first-generation steels. The Q&P heat treatment process was first developed by Speer et al. in 2003 to produce high-strength third-generation steels for a high-speed car chassis. This process has attracted a lot of attention in the last two decades due to the improvement of mechanical properties through the creation of smart microstructure. Steels processed in this process are promising candidates for industries [7, 8].

This category of steel includes high-strength phases (martensite, bainite, or fine-grained ferrite) and a significant amount of the austenite phase. Achieving high ultimate tensile strength and formability hinges on the presence of a certain amount of residual austenite in the microstructure of steel in the form of nano-sized layers. Therefore, the main challenge in producing this generation of steel is stabilizing the remaining austenite phase in the final structure. Notably, austenite is thermodynamically unstable at room temperature and can transform into martensite under high strain conditions [9, 10].

Many researchers have used this process to develop thin steel sheets with different fractions of martensite and residual austenite. This process fundamentally requires partial or full austenitization of the material; the choice of each depends on the expected mechanical properties. Rapid cooling is then performed below the martensite start temperature (M_s) and above the martensite finish temperature (M_f) to create a controlled

volume fraction of supersaturated martensite and untransformed austenite. During a single-stage operation at the quenching temperature or in a two-stage operation above the initial quenching temperature, carbon penetrates from martensite into austenite (carbon partitioning). The part is then cooled to ambient temperature [11]. Three factors are crucial for the stability of austenite at room temperature: the chemical composition of the steel, the size and morphology of the austenite, and its surrounding phases [12-14]. Carbon, an inexpensive stabilizing element, enhances austenite stability by penetrating from supersaturated martensite into austenite during the partitioning phase [15]. Room-temperature-stabilized austenite effectively contributes to the properties of ferrous alloys, especially low-alloy steels whose properties have always been affected by austenite instability at room temperature [16]. The residual austenite stability prevents shape changes due to temperature fluctuations or tension during service [17]. A martensitic matrix containing more than 5% residual austenite by volume fraction improves the material's plasticity [4]. Processed Q&P steels with a martensite matrix can be strengthened by the stabilized austenite phase transformation, making them ideal candidates for wear and impact resistance applications in modern engineering equipment [18-21]. Generally, controlling the volume fraction of stabilized (retained) austenite requires an accurate design of the quenching and partitioning time and temperature, which has a great effect on the chemical components and morphology of the steel to improve its performance [22].

The literature evaluates the effects of different Q&P process parameters across a wide range of steels. Efforts have been made to achieve higher mechanical properties by identifying optimal quenching temperatures and partitioning heat treatments for each steel type. For example, applying the Q&P process to low-carbon steel has resulted in a yield strength of 1047 MPa and a relative elongation of 15.5%. Studies on low- and medium-carbon steels indicate that the use of the Q&P process enhances strength while maintaining an acceptable relative elongation [23, 24].

Jirková et al. [25] investigated the effect of

partitioning temperature on the mechanical properties of three low alloy steels with different Si and Mn contents. Their finding showed that an increase in partitioning temperature in all cases reduced strength and increased toughness due to martensite tempering at higher temperatures. Additionally, higher partitioning temperature causes stability of the retained austenite fraction. They also observed that the ultimate tensile strength of the steel gradually decreased as partitioning time increased, whereas yield strength first decreased and then increased with longer partitioning time.

Despite numerous studies on the effect of the Q&P process on microstructural changes and the mechanical properties of different steels, no statistical investigation of process factors and their effects on 1.7102 steel has been conducted to date. Therefore, this research, using a scientific full factorial design of experiments, investigates the effect of the Q&P process on the mechanical properties of steel bars made of 1.7102 medium carbon steel. While previous studies have qualitatively examined the effect of process factors on the mechanical properties of various steels, the objective of the present study is to quantitatively analyze the effects of each factor on the mechanical properties of 1.7102 steel.

Therefore, the results are discussed and interpreted using the statistical analysis of variance (ANOVA) method. It is worth noting that the statistical analysis in this research is applied to the experimental results presented in the authors' previous studies [1, 23].

2. Materials and Methods

In this study, medium carbon steel 1.7102 (54SiCr6) with a diameter of 10 mm was used. The chemical composition of the test specimen was determined by atomic emission spectroscopy, as shown in Table 1. To determine the optimal quenching and partitioning temperatures, the critical temperatures of the steel were obtained from JMatPro software, with the results reported in Table 2. The investigated variables in the heat treatment process are partitioning time (Pt) and quenching temperature (QT). Test specimens, each 120

mm in length, were kept at 900 °C for 20 minutes, as illustrated in the cycle shown in Fig. 1 for complete austenitization. They then underwent the designed heat treatment process. No tempering was performed on the specimens. Oil was used as the quenching environment.

The samples were labeled based on the quenching temperature and partitioning time; for instance, sample 230-8 refers to a specimen quenched at 230 °C and partitioned for 8 minutes. An infrared thermometer was used to measure the temperatures. After heat treatment, standard tensile test samples were prepared in accordance with ASTM E8 standards. These tensile samples had a length of 30 mm and a diameter of 6 mm. The tensile test was performed using an engineering strain rate of 10 mm/min. Additionally, a hardness test was performed on the samples with three repetitions.

The experiments were designed to evaluate the effect of process variables on ultimate tensile strength (UTS), yield strength (YS), total elongation (TEL), reduction area (RA), and hardness (HB). Two factors of quenching temperature at three levels and partitioning time at four levels were determined as shown in Table 3. A full factorial design of experiments was used, resulting in twelve experimental runs, each performed with three replications, as reported in Table 4.

Table 1. Chemical composition of the spring steel 54SiCr6 (wt.%)

C	Si	Mn	P
0.520	1.40	0.640	0.0123
S	Cr	Mo	Ni
0.0039	0.621	0.0024	0.0416

Table 2. Critical temperatures of steel (°C)

Ms	Mf	AC1	AC3
286	164	723	837

Table 3. Input parameters (variables) and their levels

Factors	Level 1	Level 2	Level 3	Level 4
QT (°C)	170	200	230	*
Pt (min)	3	8	15	30

3. Results and Discussion

This study investigated the effects of quenching temperature and partitioning time on the mechanical properties of 1.7102 carbon steel.

Table 4. Effects of QT (°C) and Pt (min) on responses

QT (°C)	Pt (min)	UTS (MPa)	YS (MPa)	RA (%)	TEL (%)	Hardness (HB)
230	3	1963.90	1898.50	31.580	12.6500	585.500
230	3	1981.14	1897.73	30.650	13.5938	587.918
230	3	1953.96	1889.27	29.701	11.4563	584.403
200	3	2046.20	1995.30	42.410	9.9950	571.500
200	3	2036.14	1981.13	43.060	9.8925	566.704
200	3	2043.28	1983.67	43.732	10.0663	571.318
170	3	1917.70	1608.17	42.900	7.9800	578.500
170	3	1934.64	1614.63	39.801	8.5913	576.385
170	3	1899.76	1600.40	42.740	7.6996	581.633
230	8	1942.50	1789.60	18.020	10.1500	588.400
230	8	1929.56	1782.83	19.020	8.9563	593.841
230	8	1958.44	1754.37	18.750	9.0337	587.841
200	8	2007.30	1698.07	20.102	8.9000	630.980
200	8	2021.24	1699.53	22.710	9.6788	626.981
200	8	1999.36	1700.30	20.550	8.5840	631.650
170	8	1973.30	1683.43	31.620	10.3000	574.300
170	8	1991.24	1664.97	28.740	10.4012	570.213
170	8	1956.36	1680.20	31.423	9.7043	576.741
230	15	1931.80	1826.60	30.450	10.4000	568.300
230	15	1973.94	1817.83	31.970	9.9050	563.708
230	15	1945.06	1867.37	32.440	9.9802	570.917
200	15	1821.40	1624.87	20.234	10.1000	590.356
200	15	1852.34	1664.33	20.000	10.0837	588.549
200	15	1798.46	1647.10	18.000	9.7415	592.005
170	15	1827.84	1525.90	45.200	10.2000	571.325
170	15	1836.90	1547.13	48.300	12.1800	571.650
170	15	1828.96	1521.67	46.320	10.5024	575.004
230	30	1942.50	1679.60	22.150	8.9000	529.860
230	30	1973.56	1748.83	22.000	8.9600	529.323
230	30	1954.44	1689.37	20.280	8.4228	536.580
200	30	1981.50	1733.67	43.350	7.6500	545.012
200	30	1991.44	1774.13	45.600	8.2475	540.902
200	30	1971.56	1748.90	42.332	7.4073	547.557
170	30	1975.90	1692.00	48.990	7.5000	568.201
170	30	1981.84	1712.23	49.947	8.0062	566.513
170	30	1961.96	1700.77	49.438	7.2337	571.650

In the Q&P process, these mechanical properties depend on process parameters such as quenching temperature and partitioning time, making it crucial to determine the optimal values for each factor. The main objective was to investigate the effects of important and

effective factors during the Q&P process, including two parameters of quenching temperature and partitioning time. To achieve this, the experimental results were statistically analyzed using Minitab software.

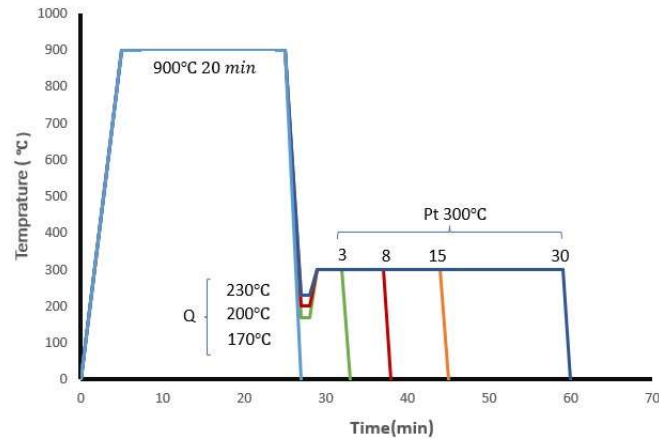


Fig. 1. Schematic of the Q&P cycles [1].

Definitive conclusions regarding the influence of these parameters were drawn through analysis of variance (ANOVA), which assumes normal data, Gaussian error distribution, and constant variance. Before conducting ANOVA, the null hypothesis for the experimental data was tested to ensure the validity of these assumptions. Once these assumptions were confirmed, the variance analysis results were deemed reliable. A 95% confidence level was adopted in this study, meaning the P-values below 0.05 indicate a significant effect of the input parameters on the response. The results showed that the selected parameters and their interactions have different effects on the responses.

3.1. Ultimate tensile strength

In the Q&P process, an increase in the martensite volume fraction enhances the material's strength. Partitioning time has a decisive role in the amount of carbon residue in martensite or its degree of tempering, both of which have a significant effect on the final tensile strength. The ANOVA results for final tensile strength are presented in Table 5. A P-value below 0.05 indicates a statistically significant effect of a factor on the response. Among the investigated factors, partitioning time had the greatest effect on ultimate tensile strength with a 52.82% contribution. In contrast, the effect of quenching temperature was much lower, contributing only 7.47%.

The interaction between the two factors accounted for 35.72% of the variation in ultimate tensile strength. The calculated error in the analysis was approximately 4%. The coefficient of determination (R^2) for the predicted model is 96.02%, which shows a high level of accuracy in estimation. The main effects of both parameters on ultimate tensile strength are shown in Fig. 2. The results indicate that the highest ultimate tensile strength is obtained at a quenching temperature of 200 °C.

The lowest ultimate tensile strength was obtained at the quenching temperature of 170 °C. By increasing the quenching temperature from 170 °C to 200 °C, the ultimate strength rose while it declined when the quenching temperature was further increased to 230 °C. The amount of martensite in the microstructure depends on the martensite start temperature (M_s) and finish temperature (M_f). An increase in the quenching temperature reduces the martensite fraction, and an increase in the austenite decreases the strength. Conversely, lowering the quenching temperature excessively increases the martensite fraction, leading to the creation of a hard martensitic structure that promotes crack growth, thereby reducing strength [13]. Fig. 2 shows the statistical average of ultimate tensile strength as a function of partitioning time and quenching temperature. The results show that the ultimate tensile strength of the samples increases with partitioning time from 3 to 8 minutes.

Table 5. ANOVA table for ultimate tensile strength

Source	DF	Seq SS	Contribution	Adj SS	Adj MS	F-value	P-value
Model	11	136061	96.02%	136061	12369.2	52.57	0.000
Linear	5	85440	60.29%	85440	17088.0	72.63	0.000
QT	2	10587	7.47%	10587	5293.4	22.50	0.000
Pt	3	74853	52.82%	74853	24951.0	106.05	0.000
2-Way interactions	6	50621	35.72%	50621	8436.8	35.86	0.000
QT×Pt	6	50621	35.72%	50621	8436.8	35.86	0.000
Error	24	5647	3.98%	5647	235.3		
Total	35	141707	100.00%				

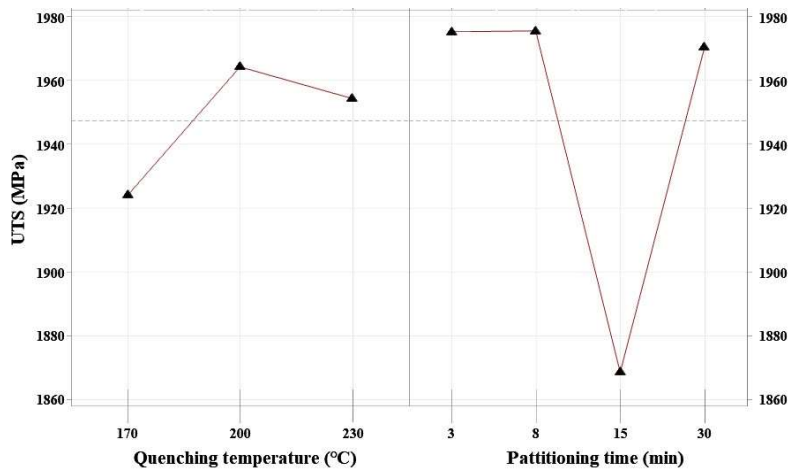


Fig. 2. Main effects of QT (°C) and Pt (min) on the ultimate tensile strength.

However, by increasing the partitioning time to 15 minutes, the ultimate tensile strength is reduced sharply. This decline is attributed to the effects of partitioning time, which causes the carbon to partition from martensite. The reduction in carbon content within martensitic leads to a decrease in strength. Thereafter, by increasing the partitioning time to 30 minutes, the ultimate tensile strength increased again. This improvement is likely due to the decomposition of unstabilized austenite into bainite, which increases the strength [19]. The highest ultimate tensile strength was obtained with a partitioning time of 8 minutes, while the lowest amount was obtained at 15 minutes of partitioning. When there is an interaction between the factors, the individual effects of each factor lose their importance, and drawing conclusions without considering these interactions lacks scientific validity. The interaction effects of the input factors on ultimate tensile strength are reported in Fig. 3. The results show that except for samples partitioned for 15 minutes, other samples have shown a similar trend: Initially, with

increasing the quenching temperature and partitioning time, the maximum tensile strength rose slightly. However, with further increases in both factors, it declined.

The regression equation for the ultimate tensile strength (UTS) as a function of partitioning time (Pt) and quenching temperature (QT) is as follows:

$$UTS (MPa) = 1852.4 + 0.506 \times QT - 0.44 \times Pt \quad (1)$$

3.2. Yield strength

Yield strength represents the stress required to start the plastic deformation. An increase in yield strength can be due to a higher volume fraction of retained austenite at elevating quenching temperature, which transforms into secondary martensite after subsequent cooling. As shown in Table 6, quenching temperature (QT) has the most significant effect on yield strength with a 38.94% contribution. Also, the interaction between quenching temperature and partitioning time (QT × Pt) has a substantial impact, contributing 36.49%, which is higher

than the individual effect of partitioning time (23.14%). The calculated error was 1.43%, and the coefficient of determination (R^2) was 98.57%.

The main effects of the parameters on yield strength are shown in Fig. 4. The obtained results show that by increasing the quenching temperature from 170 °C to 200 °C, yield strength increased dramatically, while increasing the quenching temperature from 200 °C to 230 °C had a reverse effect. The highest and lowest yield strengths were recorded for the quenching temperatures of 200 °C and 170 °C, respectively. The main effects plot shows that increasing partitioning time to 15 minutes reduces yield strength. However, further increasing the partitioning time from 15 to 30 minutes leads to an improvement in yield strength. This recovery can be attributed to carbide precipitation, which reduces the

retained austenite during the partitioning time of 30 minutes [1]. The highest yield strength was recorded at a partitioning time of 3 minutes, while the lowest was at 15 minutes. Increasing the partitioning time has reduced the residual austenite and the formation of carbide deposits, which ultimately led to a decrease in yield strength [18]. Overall, the effect of quenching temperature on yield strength was more significant than that of partitioning time.

The statistical results in Table 6 indicate that the interaction between the factors is significant. This interaction is visually confirmed in the interaction plot shown in Fig. 5, which illustrates the combined effects of quenching temperature (QT) and partitioning time (Pt) on yield strength.

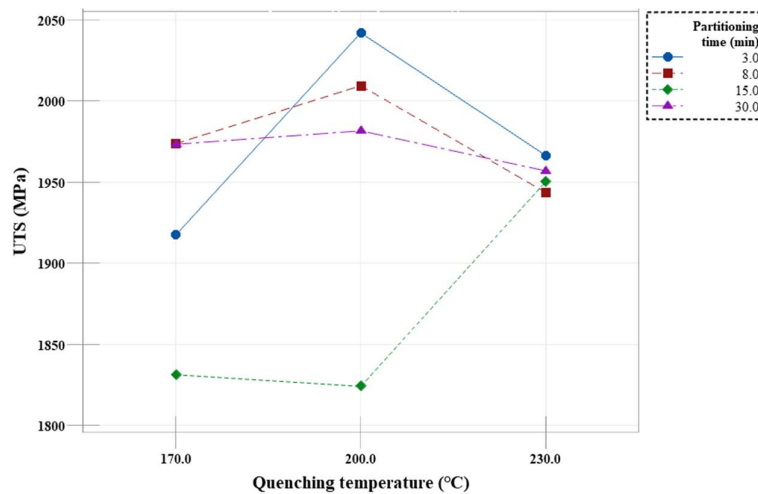


Fig. 3. The interaction of QT (°C) on the ultimate tensile strength.

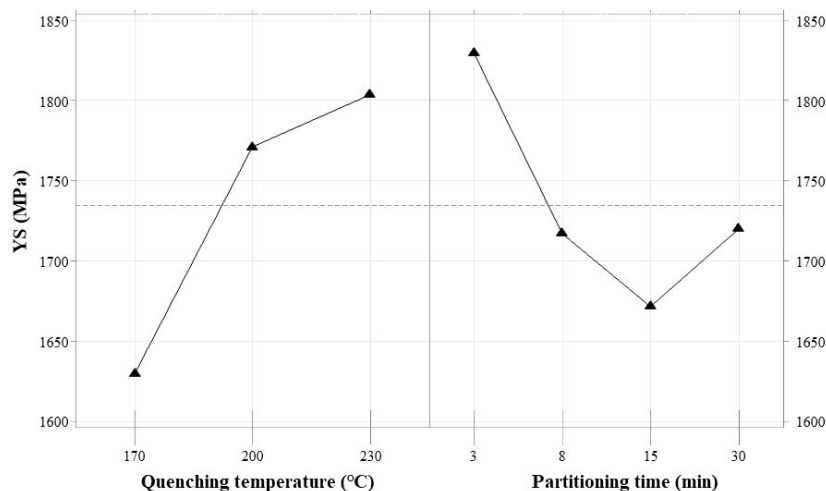


Fig. 4. Main effects of QT (°C) and Pt (min) on the yield strength.

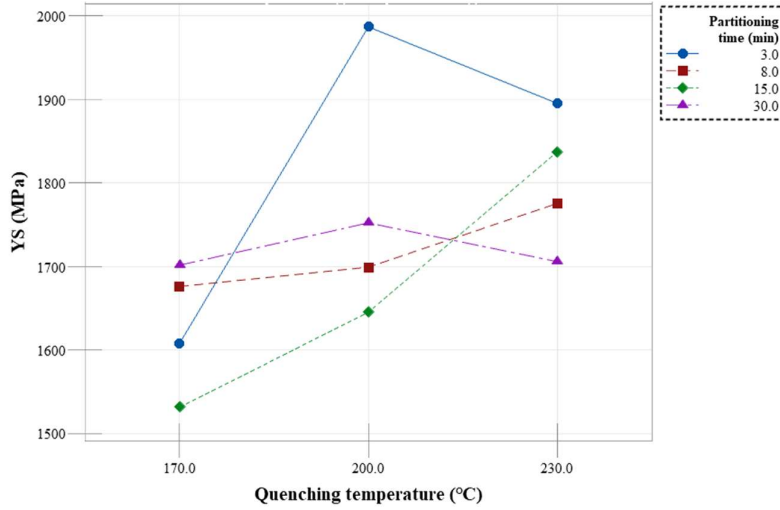


Fig. 5. The interaction of QT (°C) and Pt (min) on the yield strength.

Table 6. ANOVA table for the yield strength

Source	DF	Seq SS	Contribution	Adj SS	Adj MS	F-value	P-value
Model	11	521100	98.57%	521100	47373	150.24	0.000
Linear	5	328172	62.08%	328172	65634	208.15	0.000
QT	2	205858	38.94%	205858	102929	326.43	0.000
Pt	3	122315	23.14%	122315	40772	129.30	0.000
2-Way interactions	6	192927	36.49%	192927	32155	101.97	0.000
QT×Pt	6	192927	36.49%	192927	32155	101.97	0.000
Error	24	7568	1.43%	7568	315		
Total	35	528667	100.00%				

In general, increasing the partitioning time and quenching temperature does not show a consistent trend in their effect on yield strength. The regression equation for the yield strength was calculated in terms of the two factors, partitioning time (Pt) and quench temperature (QT), and is presented below:

$$YS (MPa) = 1196 + 2.903 \times QT - 3.00 \times Pt \quad (2)$$

3.3. Total elongation

The increase or decrease of ductility is dependent on the amount of retained austenite as a ductile phase in the microstructure. The ANOVA results for total elongation are presented in Table 7. The obtained P-values indicate the significance of the input factors and their interaction with the total elongation percentage. Partitioning time had a greater effect on total elongation (40.64% contribution) compared to quenching temperature (10.90% contribution). The contribution percentage accounted for 37.86% of the variance. The error was

10.60%, and the coefficient of determination (R^2) was 89.40%.

The main effect of each factor on the total elongation is observable in Fig. 6. The partitioning time chart reveals that increasing the partitioning time from 3 to 8 minutes results in a decrease in elongation, while further increasing the partitioning time from 8 to 15 minutes leads to an increase in elongation. The highest average total elongation occurred at a partitioning time of 15 minutes. The increase in the retained austenite delayed the growth of cracks and increased the elongation [25]. However, increasing the time from 15 to 30 minutes caused a drastic decrease in total elongation, with the lowest value recorded at 30 minutes. This can be attributed to the extended partitioning time allowing for the austenite decomposition (i.e., carbides formation), which reduces the total elongation [23]. Regarding the quenching temperature, the average elongation increased as the quenching temperature (QT) rose from

170 °C to 200 °C, but then decreased with further increases in quenching temperature.

Moreover, the highest and lowest values were recorded at 200 °C and 230 °C, respectively. According to the results, the effect of partitioning time on total elongation was more significant than the effect of

quenching temperature.

According to the significance of the interaction effect between the input parameters, the interaction plot is used to study this effect. The interaction between the input factors on total elongation is shown in Fig. 7.

Table 7. ANOVA table for the total elongation percentage

Source	DF	Seq SS	Contribution	Adj SS	Adj MS	F-value	P-value
Model	11	66.534	89.40%	66.534	6.0486	18.39	0.000
Linear	5	38.359	51.54%	38.359	7.6718	23.33	0.000
QT	2	8.114	10.90%	8.114	4.0571	12.34	0.000
Pt	3	30.245	40.64%	30.245	10.0816	30.66	0.000
2-Way interactions	6	28.175	37.86%	28.175	4.6959	14.28	0.000
QT×Pt	6	28.175	37.86%	28.175	4.6959	14.28	0.000
Error	24	7.892	10.60%	7.892	0.3288		
Total	35	74.426	100.00%				

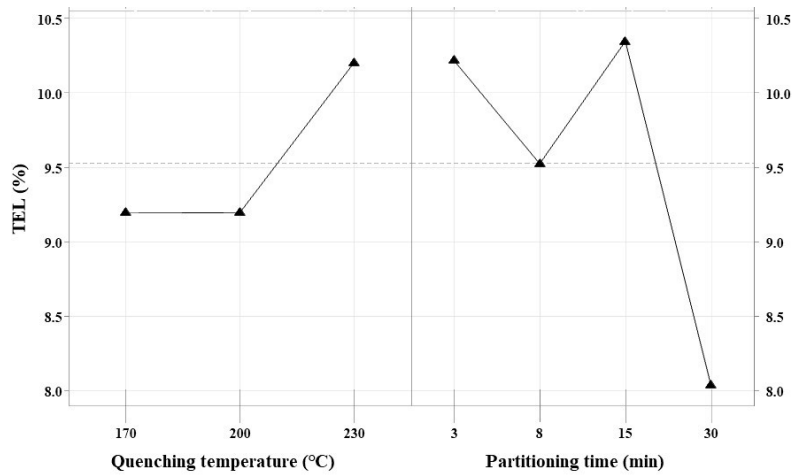


Fig. 6. Main effects of QT (°C) and Pt (min) on the total elongation percentage.

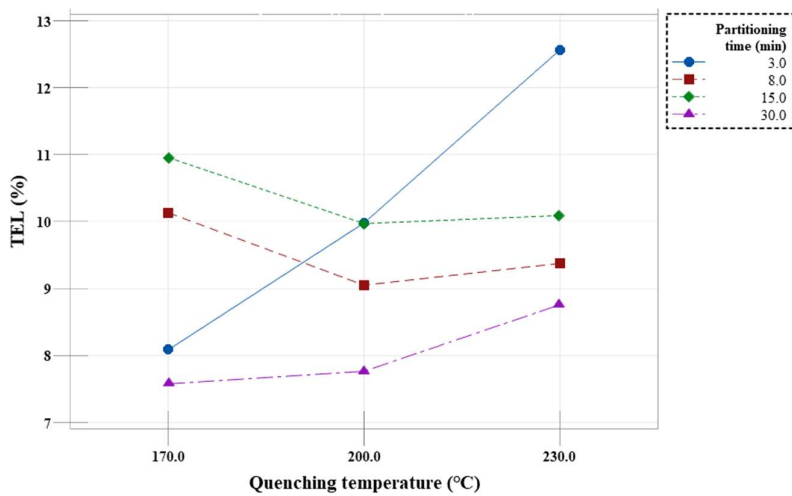


Fig. 7. The interaction of QT (°C) and Pt (min) on the total elongation percentage.

Total elongation decreases at low partitioning time and quenching temperature. However, increasing the quenching temperature and partitioning time (up to 15 minutes) results in an increased total elongation. Moreover, the lowest total elongation occurred at the highest quenching temperature and partitioning time, likely due to the formation of carbide precipitates [24]. As shown in Fig. 7, with a fixed partitioning time (except for 3 minutes), a decrease in the quenching temperature increases total elongation. Conversely, increasing the partitioning time from 8 to 15 minutes at a constant quenching temperature results in decreased total elongation. The variation in this parameter is definitely dependent on the amount of retained austenite, which serves as a ductile phase in the microstructure. Austenite films, intercalated between martensite layers, create a softer and more ductile phase compared to martensite. This configuration inhibits microcrack propagation and enhances ductility [4].

The regression equation for the total elongation was calculated in terms of the two factors, partitioning time and quenching temperature, and is presented as below:

$$TEL (\%) = 7.20 + 0.01682 \times QT - 0.0738 \times Pt \quad (3)$$

3.4. Reduction of area

The reduction of area in P&Q steels is strongly affected by quenching temperature and partitioning time. The quenching time creates a specific volume fraction of austenite and supersaturated martensite, while the partitioning time causes the release of carbon from martensite and stabilizes the austenite. To achieve good ductility, the steel must maintain nanosized layers of austenite in its martensitic matrix [22]. The ANOVA results for the reduction area are given in Table 8. Both quenching temperature (QT) and partitioning time (Pt), as well as their interaction, significantly affect the reduction of area, with contribution percentages of 38.67%, 31.05%, and 29.44%, respectively. The amount of computational error was found to be 0.86%, and the coefficient of determination (R^2) was 99.15%.

The main effects plot for each factor on the reduction area is shown in Fig. 8. The results indicate that as the

partitioning time increases from 3 to 8 minutes, the reduction area percentage decreases. However, with a further increase in partitioning time from 8 min to 30 min, the reduction area percentage shows an upward trend. This increase in partitioning time leads to martensite tempering, resulting in improved elongation and ductility [20]. From the findings, it can be concluded that the P&Q process has an optimal partitioning time where both strength and flexibility values are balanced. This observation aligns with the research conducted by Wang et al. [24]. The highest average reduction area occurred at a partitioning time of 30 minutes, while the lowest value was recorded at 8 minutes. The graph of the average reduction area as a function of quenching temperature indicates that the increase in the quenching temperature causes a decrease in the reduction area. The highest reduction area was observed at 170 °C, whereas the lowest was recorded at 230 °C.

The interaction of factors affecting the maximum reduction area is shown in Fig. 9, demonstrating a significant interaction between the input parameters.

The regression equation for the reduction of area in terms of the two factors, partitioning time (Pt) and quenching temperature (QT), is presented below:

$$RA (\%) = 85.6 - 0.2756 \times QT + 0.193 \times Pt \quad (4)$$

3.5. Hardness

The ANOVA results for the hardness are presented in Table 9. The findings confirm the significant effects of all factors and their interactions. The contribution percentages for quenching temperature, partitioning time, and their interaction effect are 37%, 45.59%, and 14.90%, respectively. According to the P-values in Table 9, the significant impact of factors on hardness is confirmed. The error value is 2.50%, and the coefficient of determination (R^2) is 96%, which indicates a high degree of model accuracy.

The partitioning process softens the martensite and reduces the hardness. The main effects of quenching temperature and partitioning time on the hardness are shown in Fig. 10. Hardness decreases as the partitioning time increases from 3 min to 8 min, which can be

attributed to carbon diffusion from martensite to surrounding austenite, thereby reducing wear resistance [26]. However, with further increase in partitioning time beyond 8 minutes, hardness increases, likely due to the formation of lower bainite [27].

An increase in quenching temperature from 170 °C to 200 °C results in higher hardness, while further increasing the quenching temperature to 230 °C causes a reduction in hardness. This reduction at higher quenching temperature (near Ms) is due to the higher volume fraction of austenite, which is softer than

martensite. The highest average hardness occurred at the quenching temperature of 200 °C and the partitioning time of 3 minutes, likely due to the limited volume fraction of the retained austenite and the presence of retained martensite in a supersaturated state [28]. Furthermore, the effect of partitioning time on hardness is greater than that of quenching temperature. In Fig. 11, the interaction of factors on hardness is reported. The contribution percentage of its effect on the hardness is 14.90%, which is significant.

Table 8. ANOVA table for the reduction of area

Source	DF	Seq SS	Contribution	Adj SS	Adj MS	F-value	P-value
Model	11	4289.12	99.15%	4289.12	389.920	255.35	0.000
Linear	5	3015.72	69.72%	3015.72	603.143	394.98	0.000
QT	2	1672.60	38.67%	1672.60	836.300	547.67	0.000
Pt	3	1343.12	31.05%	1343.12	447.706	293.19	0.000
2-Way interactions	6	1273.40	29.44%	1273.40	212.234	138.99	0.000
QT×Pt	6	1273.40	29.44%	1273.40	212.234	138.99	0.000
Error	24	36.65	0.85%	36.65	1.527		
Total	35	4325.77	100.00%				

Table 9. ANOVA table for the hardness

Source	DF	Seq SS	Contribution	Adj SS	Adj MS	F-value	P-value
Model	11	19966.5	97.50%	19966.5	1815.13	85.22	0.000
Linear	5	16914.5	82.60%	16914.5	3382.89	158.82	0.000
QT	2	7579.4	37.01%	7579.4	3789.69	177.92	0.000
Pt	3	9335.1	45.59%	9335.1	3111.69	146.09	0.000
2-Way interactions	6	3052.0	14.90%	3052.0	508.67	23.88	0.000
QT×Pt	6	3052.0	14.90%	3052.0	508.67	23.88	0.000
Error	24	511.2	2.50%	511.2	21.30		
Total	35	20477.7	100.00%				

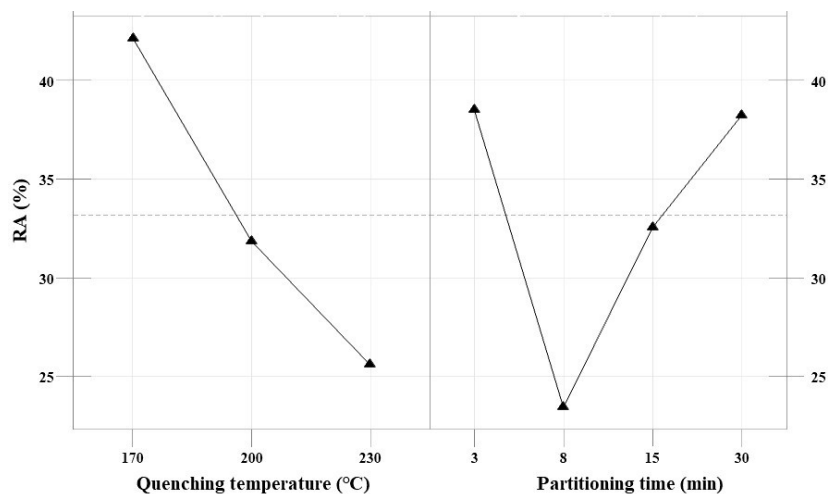


Fig. 8. Main effects of QT (°C) and Pt (min) on the reduction of area.

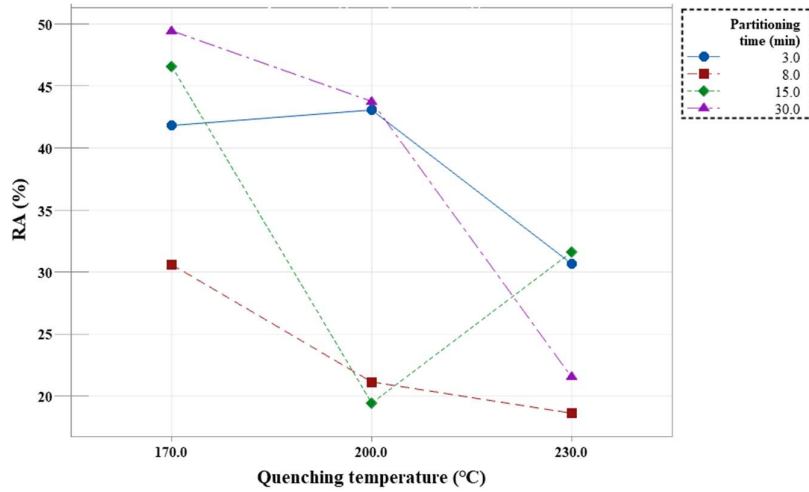


Fig. 9. The interaction of QT (°C) and Pt (min) on the reduction of area.

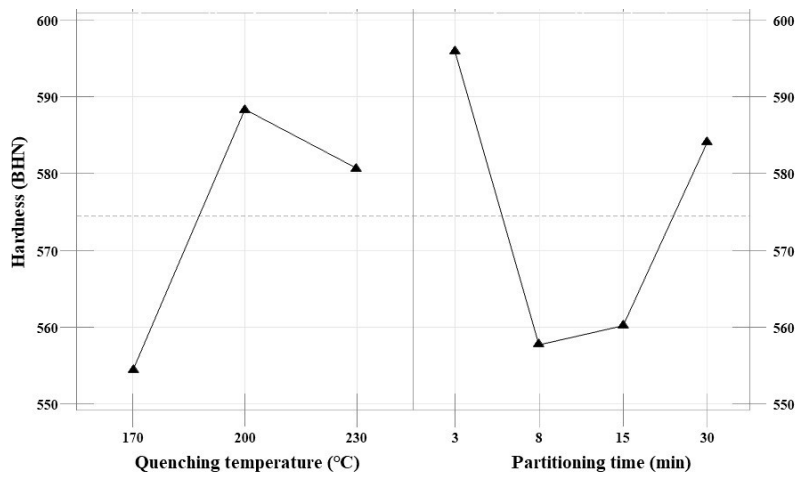


Fig. 10. Main effects of QT (°C) and Pt (min) on the hardness.

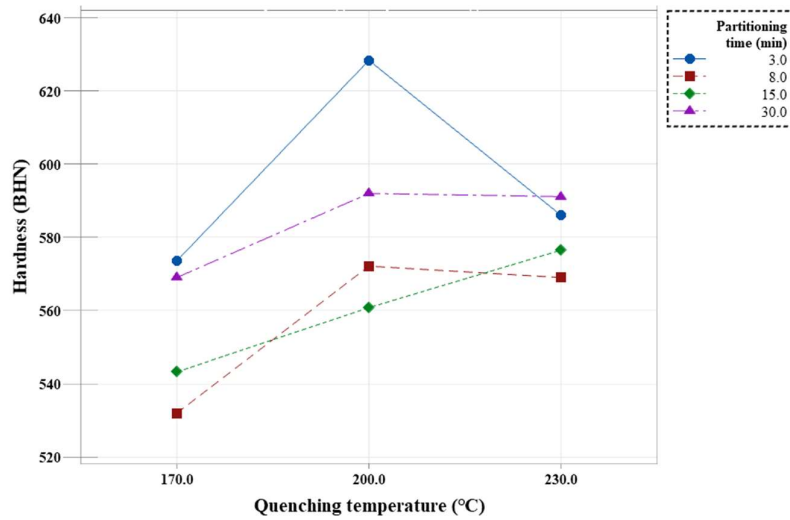


Fig. 11. The interaction of QT (°C) and Pt (min) on the hardness.

It is observed that increasing the partitioning time and quenching temperature within the range of 3 to 8 minutes reduces the hardness, while with further increase in quenching temperature and partitioning time, hardness begins to rise.

The regression equation for the hardness was calculated based on the two factors of partitioning time and quench temperature as follows:

$$\text{Hardness (BHN)} = 486.9 + 0.437 \times QT + 0.008 \times Pt \quad (5)$$

4. Conclusion

This research investigated effects and interactions of the primary factors, including the quenching temperature (at three levels) and partitioning time (at four levels), on several mechanical properties of 1.7102 silicon medium steel through statistical analysis. The findings are summarized as follows:

- Partitioning time (Pt) had the greatest effect on ultimate tensile strength (UTS) at 52.82% contribution percentage, total elongation (TEL%) at 40.64%, and hardness at 45.59%.
- Quenching temperature (QT) had the most significant effect on yield strength (YS) at 38.94% contribution percentage and reduction of area (RA%) at 38.67%.

Conflict of interest

The authors declare no conflict of interest.

Funding

The authors did not receive any financial support for the research, authorship, and/or publication of this article.

5. References

- [1] Abedini, A., Rastegari, H., & Emam, S. (2023). Mechanical properties and work hardening behaviour of spring steel after the quenching-partitioning process. *Canadian Metallurgical Quarterly*, 63(4), 1169–1182. <https://doi.org/10.1080/00084433.2023.2291288>
- [2] Gu, J., Li, D., Liu, S. & Liu, Z. (2024). Microstructure and properties of Mn–Si–Cr alloy steel modified by quenching and partitioning. *Materials Testing*, 66(3), 305-315. <https://doi.org/10.1515/mt-2023-0341>
- [3] Yu, C. J., Seo, C. H., Im, Y. R., & Suh, D. W. (2024). Influence of silicon contents on the microstructure and tensile properties of quenching and partitioning (Q&P) processed low carbon steel. *ISIJ International*, 64(2), 412-420. <https://doi.org/10.2355/isijinternational.ISIJINT-2023-113>
- [4] Wang, L., & Speer, J. G. (2013). Quenching and partitioning steel heat treatment. *Metallography, Microstructure, and Analysis*, 2, 268-281. <https://doi.org/10.1007/s13632-013-0082-8>
- [5] Diego-Calderón, I., Sabirov, I., Molina-Aldaguera, J., Föjér, C., & Thiessen, R. (2016). Microstructural design in quenched and partitioned (Q&P) steels to improve their fracture. *Materials Science & Engineering A*, 657, 136-146. <https://doi.org/10.1016/j.msea.2016.01.011>
- [6] Yang, Y., Huang, F., Guo, Z., Rong, Y., & Chen, N. (2016). Effect of retained austenite on the hydrogen embrittlement of a medium carbon quenching and partitioning steel with refined microstructure. *Materials Science and Engineering A*, 665, 76-85. <https://doi.org/10.1016/j.msea.2016.04.025>
- [7] Speer, J., Matlock, D. K., De Cooman, B. C., & Schroth, J. G. (2003). Carbon partitioning into austenite after martensite transformation. *Acta Materialia*, 51(9), 2611-2622. [https://doi.org/10.1016/S1359-6454\(03\)00059-4](https://doi.org/10.1016/S1359-6454(03)00059-4)
- [8] Bigg, T. D., Edmonds, D. V., & Eardley, E. S. (2013). Real-time structural analysis of quenching and partitioning (Q&P) in an experimental martensitic steel. *Journal of Alloys and Compounds*, 577, S695-S698. <https://doi.org/10.1016/j.jallcom.2013.01.205>
- [9] Kong, H., Chao, Q., Cai, M. H., Pavlina, E. J., Rolfe, B., Hodgson, P. D., & Beladi, H. (2018). Microstructure evolution and mechanical behavior of a CMnSiAl TRIP steel subjected to partial austenitization along with quenching and partitioning treatment. *Metallurgical and Materials Transactions A*, 49, 1509-1519. <https://doi.org/10.1007/s11661-018-4525-3>
- [10] Podder, A. S., Lonardelli, I., Molinari, A., & Bhadeshia, H. K. D. H. (2011). Thermal stability of retained austenite in bainitic steel: an in situ study. *Proceedings of the Royal Society A: Mathematical, Physical and Engineering Sciences*, 467(2135), 3141-3156. <https://doi.org/10.1098/rspa.2011.0212>
- [11] Santofimia, M. J., Zhao, L., & Sietsma, J. (2009). Microstructural evolution of a low-carbon steel during application of quenching and partitioning heat treatments after partial austenitization. *Metallurgical and Materials Transactions A*, 40, 46-57. <https://doi.org/10.1007/s11661-008-9701-4>
- [12] Santofimia, M. J., Zhao, L., Petrov, R., & Sietsma, J. (2008). Characterization of the microstructure obtained by the quenching and partitioning process in a low-carbon steel. *Materials Characterization*, 59(12), 1758-1764. <https://doi.org/10.1016/j.matchar.2008.04.004>

- [13] Wu, R. M., Li, W., Wang, C. L., Xiao, Y., Wang, L., & Jin, X. J. (2015). Stability of retained austenite through a combined intercritical annealing and quenching and partitioning (IAQP) treatment. *Acta Metallurgica Sinica (English Letters)*, 28, 386-393. <https://doi.org/10.1007/s40195-015-0217-9>
- [14] Dong, H. Y., Wu, K. M., Wang, X. L., Hou, T. P., & Yan, R. (2018). A comparative study on the three-body abrasive wear performance of Q&P processing and low-temperature bainitic transformation for a medium-carbon dual-phase steel. *Wear*, 402, 21-29. <https://doi.org/10.1016/j.wear.2018.01.009>
- [15] Liu, L., He, B. B., Cheng, G. J., Yen, H. W., & Huang, M. X. (2018). Optimum properties of quenching and partitioning steels achieved by balancing fraction and stability of retained austenite. *Scripta Materialia*, 150, 1-6. <https://doi.org/10.1016/j.scriptamat.2018.02.035>
- [16] Li, S., Zhu, R., Karaman, I., & Arróyave, R. (2013). Development of a kinetic model for bainitic isothermal transformation in transformation-induced plasticity steels. *Acta Materialia*, 61(8), 2884-2894. <https://doi.org/10.1016/j.actamat.2013.01.032>
- [17] Allain, S. Y. P., Geandier, G., Hell, J. C., Soler, M., Danoix, F., & Gouné, M. (2017). In-situ investigation of quenching and partitioning by high energy X-ray diffraction experiments. *Scripta Materialia*, 131, 15-18. <https://doi.org/10.1016/j.scriptamat.2016.12.026>
- [18] Sabirov, I., Santofimia, M. J., & Petrov, R. H. (2021). Advanced high-strength steels by quenching and partitioning. *Metals*, 11(9), 1419. <https://doi.org/10.3390/met11091419>
- [19] Hafeez, M. A. (2021). Microstructural and mechanical properties of one-step quenched and partitioned 65Mn steel. *Arabian Journal for Science and Engineering*, 46(3), 2261-2267. <https://doi.org/10.1007/s13369-020-05075-4>
- [20] Li, Q., Zhang, Y., Li, W., Huang, X., & Huang, W. (2020). Improved mechanical properties of a quenched and partitioned medium-carbon bainitic steel by control of bainitic isothermal transformation. *Journal of Materials Engineering and Performance*, 29, 32-41. <https://doi.org/10.1007/s11665-020-04554-x>
- [21] Aoued, S., Danoix, F., Allain, S. Y., Gaudez, S., Geandier, G., Hell, J. C., Soler, M., & Gouné, M. (2020). Microstructure evolution and competitive reactions during quenching and partitioning of a model Fe-C-Mn-Si alloy. *Metals*, 10(1), 137. <https://doi.org/10.3390/met10010137>
- [22] Gouné, M., Danoix, F., Allain, S., & Bouaziz, O. (2013). Unambiguous carbon partitioning from martensite to austenite in Fe-C-Ni alloys during quenching and partitioning. *Scripta Materialia*, 68(12), 1004-1007. <https://doi.org/10.1016/j.scriptamat.2013.02.058>
- [23] Abedini, A. A., Koopaei, H. R., & Emam, S. M. (2022). The Effect of quenching and partitioning process on the microstructure and tensile properties of a medium carbon high silicon steel. *Journal of Metallurgical and Materials Engineering*, 33, 59-72. <https://doi.org/10.22067/jmme.2022.74973.1039>
- [24] Wang, X. D., Zhong, N., Rong, Y. H., Hsu, T. Y., & Wang, L. (2009). Novel ultrahigh-strength nanolath martensitic steel by quenching-partitioning-tempering process. *Journal of Materials Research*, 24(1), 260-267. <https://doi.org/10.1557/JMR.2009.0029>
- [25] Jirková, H., Kučerová, L., & Mašek, B. (2012, January). Effect of quenching and partitioning temperatures in the QP process on the properties of AHSS with various amounts of manganese and silicon. In *Materials Science Forum* (Vol. 706, pp. 2734-2739). Trans Tech Publications Ltd. <https://doi.org/10.4028/www.scientific.net/MSF.706-709.2734>
- [26] Zinsaz-Borujerdi, A., Zarei-Hanzaki, A., Abedi, H. R., Karam-Abian, M., Ding, H., Han, D., & Kheradmand, N. (2018). Room temperature mechanical properties and microstructure of a low alloyed TRIP-assisted steel subjected to one-step and two-step quenching and partitioning process. *Materials Science and Engineering: A*, 725, 341-349. <https://doi.org/10.1016/j.msea.2018.04.042>
- [27] Nayak, S. S., Anumolu, R., Misra, R. D. K., Kim, K. H., & Lee, D. L. (2008). Microstructure-hardness relationship in quenched and partitioned medium-carbon and high-carbon steels containing silicon. *Materials Science and Engineering: A*, 498(1-2), 442-456. <https://doi.org/10.1016/j.msea.2008.08.028>
- [28] Santofimia, M. J., Zhao, L., & Sietsma, J. (2011). Overview of mechanisms involved during the quenching and partitioning process in steels. *Metallurgical and Materials Transactions A*, 42, 3620-3626. <https://doi.org/10.1007/s11661-011-0706-z>